ADVANCED ENGINEERING MATERIALS

DOI: 10.1002/adem.201400524

Lightweight Metal Cellular Structures Fabricated via 3D Printing of Sand Cast Molds**

By *Dean Snelling,* Qian Li, Nicolas Meisel, Christopher B. Williams, Romesh C. Batra* and *Alan P. Druschitz*

Cellular structures offer high specific strength and can offer high specific stiffness, good impact absorption, and thermal and acoustic insulation. A major challenge in fabricating cellular structures is joining various components. It is well known that joints, either welded or bolted or bonded with an adhesive, serve as stress concentrators. Here, we overcome this shortcoming by the use of metal casting into 3D printed sand molds for fabricating cellular structures and sandwich panels. Furthermore, the use of 3D printing allows for the fabrication of sand molds without the need for a pattern, and thus enables the creation of cellular structures with designed mesostructure from a bevy of metal alloys. We use the finite element method to numerically analyze the energy absorption capabilities of an octet truss cellular structure created with the proposed manufacturing process and that of a solid block of the same material and area density as the cellular structure. In the numerical simulations, mechanical properties collected through experimental quasi-static compression testing are employed. It is found that indeed the cellular structure absorbs considerably more impact energy over that absorbed by a solid structure of the same weight.

1. Motivation

As military vehicles and infrastructure face ever-increasing lethal threats, there is continued interest for lightweight ballistic armor that will improve vehicle performance and safety and decrease vehicle transportation costs. Cellular materials (metallic bodies with inter-dispersed voids) are a promising class of structures for addressing this need. Cellular materials offer high strength accompanied by low density[1] and can offer high stiffness, good impact-absorption, and thermal and acoustic insulation.[2]

Recent cellular material research has focused on designing the mesoscopic topology (the geometric arrangement of the solid phases and voids within a material or product of the size range 0.1–10 mm) in order to effectively support and improve multiple design objectives.[3–5] Example applications of designed cellular mesostructure include a jet engine combustor liner that has sufficient strength to withstand extreme pressures and stresses from thermal expansion while still maintaining open cells that allow for active cooling via forced convection and a lightweight blast-resistant panel that efficiently absorbs impact from large impulse forces.[6–9]

Due to their complex internal geometry, manufacturing a component with cellular mesostructure is impossible with traditional subtractive machining. As such, researchers have looked to advanced manufacturing technologies to produce this unique class of materials.

1.1. Traditional Cellular Material Manufacturing Methods

Stochastic metal foaming processes feature generating gas in liquid metal (Alporas, Hydro/Alcan/Combal, Gasar/Lotus processes), or by mixing metal powders with a blowing agent which is then compacted and melted (Alulight/Foaminal techniques). [2] While these processes result in structures with cells of random shape, morphology, and distribution,[10] they "place material in locations where it

[*] *Dr. D. Snelling, N. Meisel, Prof. C. B. Williams*
Department of Mechanical Engineering, Design, Research, and Education for Additive Manufacturing Systems Laboratory, Virginia Polytechnic Institute and State University, 410 Goodwin Hall, 635 Prices Fork Road, Blacksburg, VA 24061, USA
E-mail: snelling@vt.edu
Q. Li, Prof. R. C. Batra
Department of Biomedical Engineering and Mechanics, Virginia Polytechnic Institute and State University, Blacksburg, VA 24061, USA
Prof. A. P. Druschitz
Department of Material Science and Engineering, Virginia Tech Foundry Institute for Research and Education, Virginia Polytechnic Institute and State University, Blacksburg, VA 24061, USA

[**] *The authors gratefully acknowledge the financial support received from the Institute for Critical Technology and Applied Science (ICTAS) at Virginia Tech.*
The affiliations were corrected after initial online publication.

contributes little to material properties (other than density). "[4] The largest limitation of stochastic cellular structures is the complete lack of control that a designer has over the topology of the mesostructure; the techniques do not provide repeatable, or even predictable, results.[1] Furthermore, these techniques limit a designer in the types of macrostructure that can be produced.

Ordered cellular structures are characterized by a periodic unit cell or by a repeating structure throughout the part and are, therefore, predictable as compared to stochastic materials. Compared to stochastic materials, ordered structures have superior mechanical properties, including energy absorption, strength, and stiffness.[11] Ordered cellular materials have been made by stamping or crimping thin sheets of metal into a corrugated shape and then joining them to create periodic structures.[8] Alternatively, they have been created by joining and bonding slotted metal sheets,[12] extrusion and electro-discharge machining,[9] and weaving and brazing metal filaments to form a periodic textile.[13,14] In the early 2000 s, Jamcorp Inc. explored the use of sand casting to process lattice block materials (LBMs). [15] The company used specially made preforms to create trussed structures. Due to the difficulty in fabricating complex patterns for creating the sand molds, the resulting parts had a planar macrostructure and a fixed (pyramidal) mesostructure. To alleviate these geometric constraints, the company also investigated casting of LBMs. However, the resulting components suffered from porosity due to the inability of the fluid to access all parts of the truss structure.[8,16] Although these fabrication techniques for producing ordered cellular structures offer repeatable part quality, they limit the macrostructure of resulting parts to planar geometries,[17] and constrain a designer to the use of a specific homogeneous mesostructure throughout a part.

1.2. Context: Producing Cellular Materials via 3D Printing and Sand Casting

While the aforementioned manufacturing techniques are capable of producing cellular materials, they in some way limit designer's ability to selectively prescribe the location of material throughout the part in order to achieve optimal performance. An ideal cellular material manufacturing technique would enable the creation of any part macrostructure and mesostructure across the entire part volume. With this as an overall goal, we introduce a cellular material manufacturing process chain that incorporates 3D printing and sand casting. Specifically, the authors' process entails use of Binder Jetting Additive Manufacturing (AM; also referred to as "3D printing" or 3DP) technology to first print a cellular sand mold, which is then used in a sand casting operation, resulting in a cast metal cellular artifact.

Previous efforts in using AM to fabricate cellular materials are reviewed in Section 2. An overview of the authors' hybrid 3DP/casting process chain is presented in Section 3. A sample part geometry – a sandwich panel featuring an octet truss unit cell – is presented as a case study to illustrate (i) geometric freedom chain and (ii) structural performance of designed and fabricated components that can be made by the process chain. Experimental results of quasi-static tests on manufactured artifact and results of numerical simulations of the impact response of cellular and solid structures are provided in Section 4. Preliminary results for impact numerical simulation of the octet truss sandwich panel are described in Section 5. Finally, closure and future work is offered in Section 6.

2. Fabricating Cellular Materials via Additive Manufacturing

Given the existing limitations of cellular material manufacturing processes, and the design constraints that they impose on the resultant cellular parts, the goal of this work is to develop a manufacturing process capable of producing metallic cellular structures with designed mesostructure. To achieve this goal, we use AM for providing the design freedom needed to overcome existing manufacturing processes' limitations.

2.1. Introduction to Additive Manufacturing (AM)

The AM provides freedom of design in creating complex parts by building them in a layer by layer fashion. In the AM process, a part is modeled in a computer-aided design (CAD) program and exported as a .stl file. The file is then imported into slicing software and divided into layers. Additionally, the software determines the correct location of support material for overhanging structures. After the part is printed, the 3D object is removed for use.

2.2. AM and Metal Casting Hybrid Processes

To address the geometric constraints imposed by traditional casting and pattern fabrication, a few hybrid manufacturing processes have been proposed. In these processes, AM techniques are used to fabricate polymer patterns, which are then used to create ceramic molds for metal casting. For example, Hattiangadi and Bandyopadhyay employed Fused Deposition of Ceramics (FDC) to produce geometrically complex ceramic molds for casting with metal.[18] Similarly, Chiras *et al.* used AM to create truss structure patterns for investment casting process with a high fluidity Be–Cu alloy.[19] In addition to extrusion, Material Jetting AM (3D Systems' Multi-Jet Modeling) has been used to fabricate wax patterns for a lost-wax casting technique to fabricate complex heat exchanger designs.[20]

By combining AM and investment casting, metallic complex cellular structures can be developed with designed mesostructure. However, such processes have following limitations: *Scale:* Current AM systems are limited in their build volume and many of the recently proposed cellular structures are only able to create a single build layer.

- *Burnout:* Materials used in the AM process are not suitable for the burnout process in investment casting. For example, photopolymer from the Multi-Jet Modeling and Stereolithography processes have much higher thermal expansion than traditional wax, and typically result in cracked investment molds.

- *Cleaning and Cost:* The ceramic slurry used for investment casting can be difficult to remove from the cellular materials' intricate geometries, and in many cases requires chemically leaching residual material from the final part, which increases the cost.

2.3. Fabricating Metallic Cellular Materials with Direct-Metal Additive Manufacturing

Direct-metal AM processes, which selectively scan an energy source, such as a laser or an electron beam spot over a metal powder bed, are capable of fabricating fully dense metal artifacts without the need for additional post-processing. Selective Laser Melting,[21,22] Electron Beam Melting,[23,24] and Direct-Metal Laser Sintering[25] have all been employed in research targeted toward fabricating cellular materials. For example, Yang *et al.* created auxetic lattice structures with electron beam melting using Ti-6Al-4V.[26] Four designs were tested in compression to compare the effect of density and Poisson's ratio on strength and modulus. These results were found to compare well with predictions from analytical models for auxetic structures.

While these processes have been successfully used to fabricate parts with cellular geometries, their ability to make parts of designed mesostructure is limited by the following inherent process constraints:[27]

- *Limited Material Selection*: Direct-metal AM processes have a limited set of working materials; for example, aluminum alloys are challenging to process due to high thermal conductivity and high optical reflectivity.
- *Residual Stresses and Support Structures*: Fabricated parts also suffer from residual stresses[28,29] and/or require the use of support structures or anchors when fabricating large parts with significant overhanging geometries.[30] The required use of support scaffolds (which must be manually removed later) is especially limiting when trying to create large cellular geometries, as they would be difficult to remove from the interior cells.
- *Cost and Throughput:* These processes are relatively expensive and have a low throughput due to their use of a 1D energy patterning mechanism (i.e., a laser).
- *Part Size*: Due to the difficulty in effectively managing the thermal loads in a powder bed, direct-metal powder bed fusion AM techniques are not capable of fabricating cellular structures of a large scale. The largest build box on a commercially available machine is $40 \times 40 \times 40$ cm^3. This prevents these technologies from fabricating large-scale cellular materials that would be well suited for applications such as vehicle armor.

2.4. Fabricating Metallic Cellular Materials via Binder Jetting Patternless Sand Molds

Binder Jetting is an AM technology that creates artifacts through the deposition of binder into a powder bed of raw material. Once a layer has been printed, the powder feed piston rises, the build piston lowers, and a counter-rotating roller spreads a new layer of powder on top of the previous layer. The subsequent layer is then printed and is stitched to the previous layer by the jetted binder. A schematic of the Binder Jetting AM process is given in Figure 1. By selectively printing binder into a bed of foundry sand layer-by-layer, Binder Jetting can be used to directly fabricate molds for metal casting. As with all AM processes, 3DP offers tremendous design freedom for altering mold geometry; with this technology, molds can be fabricated with integrated gating systems, embedded cores, and without the need for a pattern. The technology is commercially offered by ZCorp's ZCast material,[31] ExOne's S-Max and M-Flex machines,[32,33] and VoxelJet.[34] Direct digital fabrication of sand molds for casting eliminates the costs associated with pattern tooling and is thus ideal for low volume production.[35,36]

Binder Jetting is a suitable AM process for the fabrication of complex cellular geometries when compared to other AM processes. These factors include the following:

- *Scalability:* The use of 2D material deposition (i.e., large inkjet print heads) provides relatively short build times when compared to other 1D deposition processes (e.g., powder bed fusion direct-metal processes).
- *Modular Molds:* Molds created from the Binder Jetting process provide the ability to be modular, meaning they can be built and assembled to create a larger homogeneous metal part.
- *Wide Range of Materials*: Any castable metal compatible with molding materials may be used for the creation of parts. For example, silica sand and furan binder used in ExOne technology can withstand materials with temperatures up to cast steel. Additionally, because this is an indirect process, other materials, such as refractories with much higher melting points, may be introduced into the mold during casting.

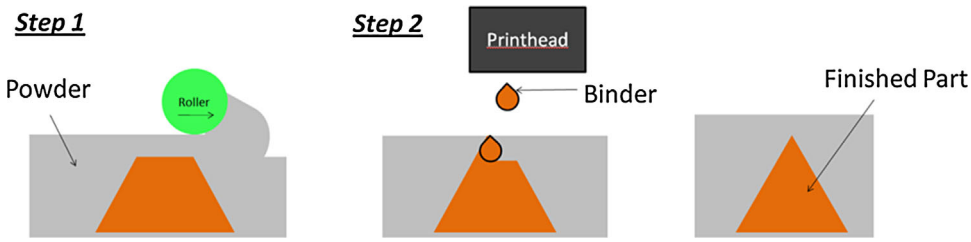

Fig. 1. Schematic of Binder Jetting AM process.

- *Microstructure Control*: Binder Jetting gives the user the potential to control microstructure of materials through better control of heat transfer by use of chills or varying wall thickness of outer molds.
- *Mold Package Optimization:* Producing molds via Binder Jetting combined with solidification modeling, permits the user to optimize metal flow for better quality castings – for example, by creating a hyperbola shaped down-sprue to decrease the chance of turbulent entrainment while pouring[37] and thus defects in castings. In contrast, the properties of direct-metal suffer from residual stresses due to large thermal gradients during the manufacturing process which are difficult to predict.
- *Support Material Constraints:* There is no need for a separate support material that must be removed in post-processing.[38] Overhanging structures are supported by the unbound powder within the powder bed during fabrication. Once the printing is complete, the unbound powder is removed from the printed part using compressed air or vacuum.

Existing research on the use of Binder Jetting for metal casting has been primarily focused on case studies and determining properties of resultant materials.[39–43] The technology has been shown to be effective in obtaining cast prototypes with dimensional tolerances that are consistent with metal casting processes.[44] AM technologies have been used in foundry practice to produce patterns and core boxes for sand casting.[45] In addition, AM processes have enabled the direct production of sand molds without the need for fabricating a pattern. In the authors' previous work, proof-of-concept cellular structures were successfully produced using ZCorporation printer and ZCast sands.[46] From this initial exploration, it was discovered that the resultant castings suffered from large voids due to off-gassing of the large amount of printed binder. In this paper, the authors report on the results from the use of a refined process chain, which features a sand system with significantly less binder (as analyzed in previous work[47]), and thus less off-gassing. In addition, the results of analytical impact and quasi-static modeling and experimental quasi-static tests on realized parts are reported. In addition to the work by the authors, studies in which part complexity is explored are limited to case studies in which existing products are cast with redesigned mold and core shapes.[48,49]

3. Binder Jetting of Sand Casting Molds for Cellular Material Fabrication

The proposed procedure for creating cast metal parts with a designed mesostructure via indirect 3D printing follows the five distinct steps: (i) digital mold design, (ii) 3D print sand mold, (iii) depowder and clean the printed mold, (iv) cast metal into printed mold, and (v) clean the cast metal part. With this process, we have been able to create a wide variety of cellular geometries from a range of castable metals. In this section, we further describe the process, and demonstrate its ability to fabricate complex cellular structures, through the creation of example part geometry: a sandwich panel with octet truss cellular structure.

3.1. Digital Mold Design

The Binder Jetting process allows for simple creation of complex mold structures from a 3D solid model. The complex mold can be designed in CAD or using software that is specialized for modeling cellular materials (e.g., netfabb's

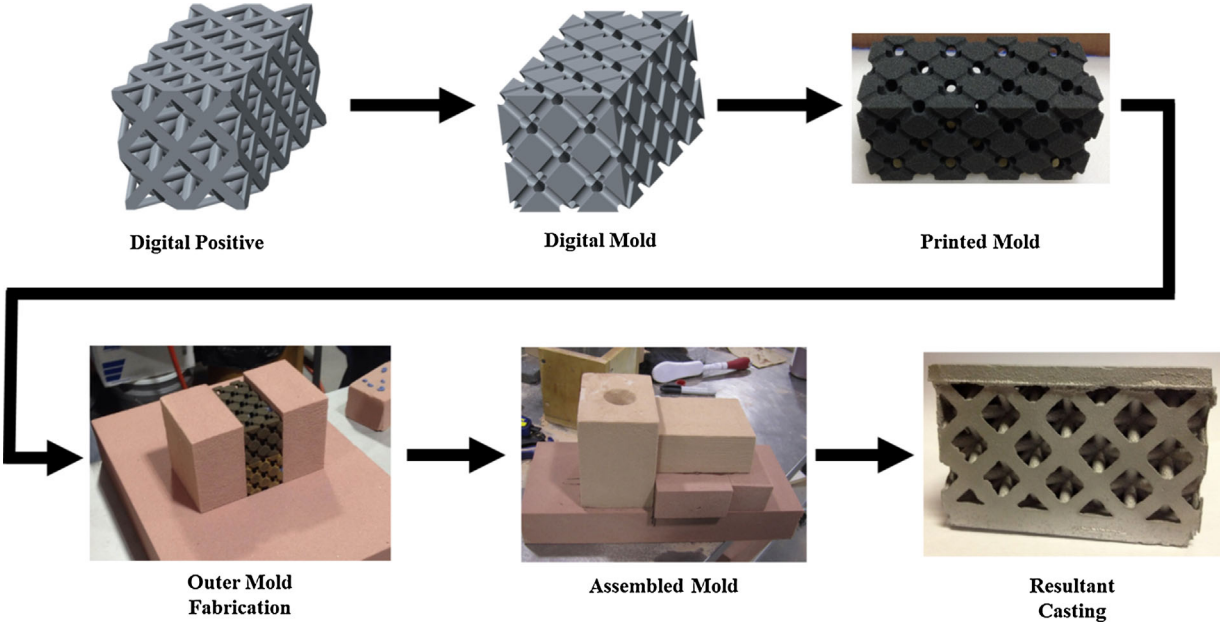

Fig. 2. Manufacturing process for creating cellular castings – from digital mold to resultant casting.

ADVANCED ENGINEERING MATERIALS

Selective Space Structures [SSS] software)[50] To create the final mold, the designed truss structure is Boolean-subtracted from a prismatic solid. An example of this process is shown in Figure 2. Using CAD, a single unit cell is designed and patterned to create the desired structure. A repeating octet truss structure is designed using netfabb SSS software; the corresponding mold is created via a Boolean subtraction from a $10 \times 5 \times 5$-mm^3 solid cube.

3.2. Mold Fabrication

With the digital creation of the mold completed, and exported to .STL format, the file is imported into the 3D printer's accompanying software, where it is oriented, scaled, and positioned. As with other powder bed processes (with direct-metal being the exception), Binder Jetting printing allows for the build volume to be completely filled with parts, thus further increasing the throughput of the process, and further improving the time-to-cast compared with traditional casting mold creation.

For this work, an ExOne S-Print machine is used for printing complex cellular molds. The ExOne technology utilizes a furan binder system which binds refined coated silica sand and has no thermal curing cycle. The silica sand is capable of casting ferrous metals, such as steel, allowing for greater variety in the final casting product. While printing, the part's atmosphere conditions including temperature and humidity are controlled in order to produce consistent molds. After printing, excess powder is vacuumed from the internal passageways of the complex mold.

Although Binder Jetting enables the direct production of entire molds, the printed molds for this example were used as sand cores, with chemically bonded sand as the casting cavity (as shown in Figure 2). An outer mold, consisting of a downsprue, gates, and runners, was formed to enable the filling of the printed mold. These mold elements direct the molten metal flow as desired, i.e., filling the printed mold from the bottom to the top. The design of the outer mold also allows for additional characteristics to be added to the desired mesostructure; in these examples, a gap between the outer mold and the printed mold creates a solid plate both above and below the designed mesostructure.

3.3. Part Creation via Metal Casting

Once the mold is formed, it can be filled with any traditional casting alloy. For this example, castings were poured in A356 alloy, a common aluminum alloy (Al-7wt%Si-0.3wt%Mg)[51] used in safety critical automotive applications due to its good combination of mechanical properties and castability. A356 ingot was melted in a SiC crucible using an electrical resistance furnace. The temperature of the metal in the furnace was limited to a maximum of about 760 °C (1400 °F); molten metal temperature was measured using an immersion thermocouple. Approximately 2 min before pouring, TiBor (Al-5wt%Ti-1wt%B) was added for grain refinement and Al-10wt%Sr was added for silicon modification. The castings were poured along with a chilled spectrometer sample for determining chemistry. The actual pouring temperature was not measured but is expected to be ~10–20 °C lower than the temperature in the furnace (actual pouring temperature: ~740–750 °C, ~1365–1380 °F).

The gating system for metal pouring was designed to fill the mold as quickly as possible and had sufficient head height to fill the complex core. A lower flow rate increases the chance of solidification before complete fill. The part was bottom-gated, and metal was fed through a one inch down sprue fabricated from the chemically bonded sand-outer mold. Castings were relatively easy to clean. Sufficient heat was available to burnout enough of the binder such that only light pressure on a pointed instrument was enough to break the mold apart. No sand burn-on or metal penetration into the mold was noted. Sand or shot blasting was not necessary to produce a clean casting.

The cleaned castings were given a standard T6 heat treatment (solution treatment followed by artificial aging) to produce a good combination of strength and ductility. The castings were heated to 540 °C (1005 °F) in an air circulating furnace and held for about 11–12 h at constant temperature to spheroidize the silicon particles and put the strengthening elements into solid solution. At the end of the high temperature cycle, the castings were removed from the furnace and quenched in a bucket of room temperature water. Next, the castings were purposely aged at 154 °C (310 °F) for 5 h. During heat treatment, the actual casting temperature was measured using a chromel–alumel thermocouple attached to the casting.

3.3.1. Metal Casting Results

Upon casting, fully homogeneous sandwiched cellular prototypes were created. Preliminary results had relied on ZCorp's Spectrum 510 for the creation of cellular structures and resulted in poor casting quality due to off-gassing associated with high binder content used for the ZCast material system. Large voids were present, producing incomplete structures and, therefore, unusable parts.[46,47] When using the ExOne system (as described in Section 3.2), resultant castings were completely filled (Figure 2) as a result of the lower binder content (~1.4%)[52].

One of the distinct advantages of cellular materials is decreased weight. The final parts produced by this method clearly demonstrate this potential reduction. The cubic piece, for example, is nominally 4297 cm^3 (262.19 in^3) in volume if the cubic space were entirely filled and there were no plates on either side of the truss section. With the ordered mesostructure, the part volume is decreased to 99.31 cm^3, only 23% of the initial volume. At a density of 2.67 g cm^{-3} for the A356 alloy, the truss part would only have a mass of approximately 265 g.

4. Quasi-Static Testing and Numerical Simulations of Deformations

To characterize mechanical properties of the cellular structure, quasi-static compression tests were performed on both solid cylinders and cellular truss structures manufactured

by the proposed Binder Jetting process. Also, quasi-static and dynamic compressive deformations of the cellular structure were numerically simulated by using the commercial software ABAQUS[53] based on the FE methodology. The computed results for quasi-static deformations are found to agree well with the corresponding experimental findings.

4.1. Quasi-Static Tests on Solid Cylinders

Six 25.4 mm long × 12.7 mm diameter cylinders of the cast material were tested under quasi-static compression. Two cellular structures, $50.8 \times 50.8 \times 50.8$ mm^3 with 6.25 mm thick face sheets, were also tested in quasi-static compression. An electromechanical testing machine (Instron) with a special compression loading fixture was employed to compress the structures at the rate of 1.5 mm min^{-1} at room temperature, and the axial load versus the crosshead displacement was recorded. The true stress versus true strain curves for the six cylinders found from the test data reveal that the curves for all six specimens are very close to each other. Young's modulus for the material was determined by fitting a straight line by the least squares method to the initial portion of the true axial stress–true axial strain curves. However, before doing so, the stress–strain curves were corrected for the initial toe regions which could be attributed to the initial slack in the loading frame. The six specimens generate a mean Young's modulus value of 20 GPa with a standard deviation of 1.1 GPa.

For numerically simulating deformations till failure of the cellular structure, we will also need stress–strain relations beyond the elastic limit. Here, we assume the material to be isotropic, homogeneous and Hookean for elastic deformations, and obeying the von Mises yield criterion with the yield stress depending only upon the effective plastic strain. The power law relationship given by Equation 1 is used to describe the strain hardening rule. In Equation 1, ϵ^{pl} is the equivalent

$$\sigma_y = A + B(\epsilon^{pl})^n \tag{1}$$

plastic strain, the parameter A equals the initial yield stress of the material, and parameters B and n described its strain hardening measured at room temperature. Values of the material parameters A, B, and n obtained by curve fitting computed values for homogeneous uniaxial compressive deformations to the experimental axial stress–axial strain curve. The parameter values are as follows: $A = 162$ MPa, $B = 355.7$ Mpa, and $n = 0.304$. Poisson's ratio of the material is taken to be 0.3, and a material point is assumed to have failed when the effective plastic strain there equals 0.5. The value of the failure strain was iteratively found till the computed axial stress–axial strain curve was found to be close to the experimental one.

4.2. Quasi-Static Tests on Cellular Structures

A photograph of the untested specimen placed in the Instron machine and that of the failed specimen are shown in Figure 3. The axial compressive load versus the axial displacement curve for the cellular structure is exhibited in Figure 4. The test results for the 1st specimen indicated that the structure can support a maximum load of 123.18 kN before trusses in the structure began to fail. The steps in the load–displacement curve are due to the incremental failure of the trusses. However, for the 2nd specimen, when the load reached 133.45 kN (Figure 4), the software in the Instron machine stopped the test before the specimen began to fail. Because of plastic deformations of the structure, it could not be re-tested.

4.3. Simulations of Quasi-Static Deformations of the Cellular Structure

Due to the symmetry of the structure and the applied boundary conditions about the two centroidal vertical planes, quasi-static deformations of only one-quarter of the structure depicted in Figure 5 were analyzed with symmetry boundary conditions applied on the plane $X = Y = Z = 0$, and the lateral surfaces kept traction-free. Two extreme cases are of infinite

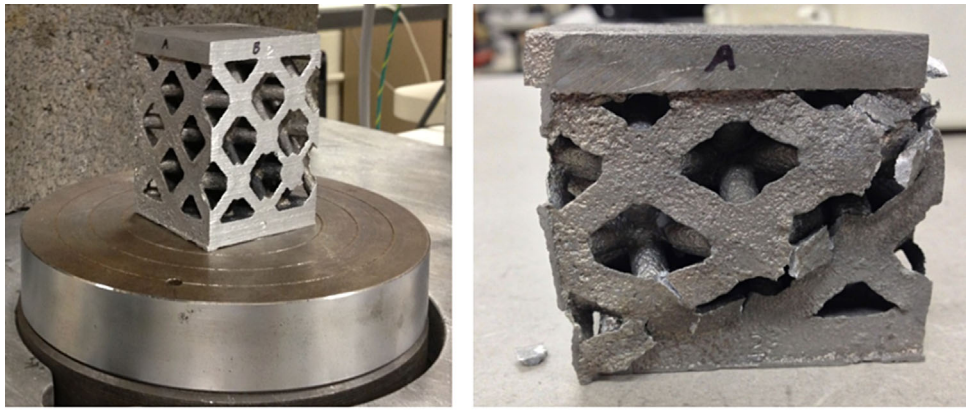

Fig. 3. Untested and failed cellular compression specimens.

ADVANCED ENGINEERING MATERIALS

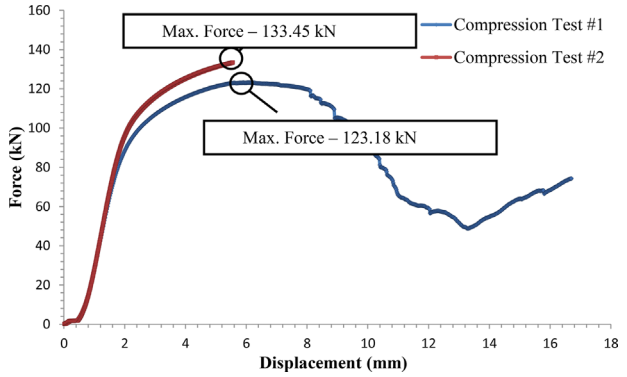

Fig. 4. Axial force versus axial displacement curve for cellular structure deformed in compression.

friction where in-plane motions of particles should be zero, and that of no friction in which case tangential tractions should be zero. In practice, the situation is somewhere between these two cases. St. Venant's principle is not applicable to the problem being studied because of large inelastic deformations involved. However, it is assumed that deformations in the central portion of the structure, away from the top and the bottom surfaces, are not affected much by boundary conditions at the contact surfaces. Therefore, lateral surfaces were assumed to be smooth and estimated that it would affect the energy dissipated by less than 5% as compared to a perfect bonding (or infinite friction) condition. Points on the bottom surface are assumed to be restrained from motion in the Z-direction and those on the top surface are incrementally moved vertically downward for a total of 10 mm. The cellular structure was discretized using 10-node tetrahedral elements with four integration points (C3D10M). The total number of the elements in the FE mesh equaled 273,828. The discretized structure is shown in Figure 5. This problem was analyzed with ABAQUS/Explicit[53] using reduced order integration rule to numerically evaluate various element matrices, and mass scaling, i.e., artificially reducing the mass density to increase the wave speed. We note that ABAQUS/Explicit analyzes dynamic problems. While checking the energy balance, the kinetic energy and the hourglass energies were found to be negligible and the total work done by external forces was found to equal the sum of the strain energy of the body and the energy dissipated due to plastically deforming the body. The general contact algorithm built in ABAQUS/Explicit was used to model contact at all interfaces including that between new surfaces formed due to element deletion. When an element has failed, both the hydrostatic pressure and the deviatoric stress components in it are set equal to zero and remain zero for the rest of the analysis.[53] The computed and the experimental true axial stress versus the true axial strain comparison curves plotted in Figure 6 differ at most by 16.4% which is taken to be within the acceptable range. Thus, values of material parameters stated above can be used to simulate deformations of the cellular structure. It is important to note that increasing the dimensional accuracy of the resultant part would eliminate error between the model and experimental results. This can be accomplished by printing the entire mold, including the outer walls otherwise made by forming traditional sand. Additionally, although compression specimens used as input data into the ABAQUS/Explicit model were cast using the same material and heat treatment, the casting modulus (Surface Area to Volume) difference between the compression specimen and proof of concept cellular structures could vary microstructure. This change in microstructure (dendrite arm spacing) will slightly affect the strength and contribute to the error.

5. Modeling Impact Loading of Cellular Structure

Transient deformations of the cellular structure due to impact loading were analyzed to delineate advantages, if any, of cellular structures over that of solid structures of the same area density. Although not optimized for blast loading, the octet truss geometry was chosen because it exhibits excellent characteristics under compressive loading and has been thoroughly studied in the literature.[54] Cellular truss structures composed of repeated unit cells have been analytically studied by analyzing deformations of a unit

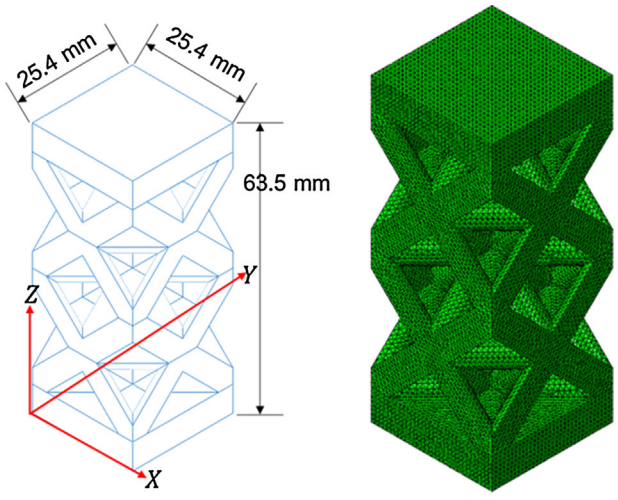

Fig. 5. Left: geometry of one quarter of the entire structure and right: its discretization into modified 10-node tetrahedral elements.

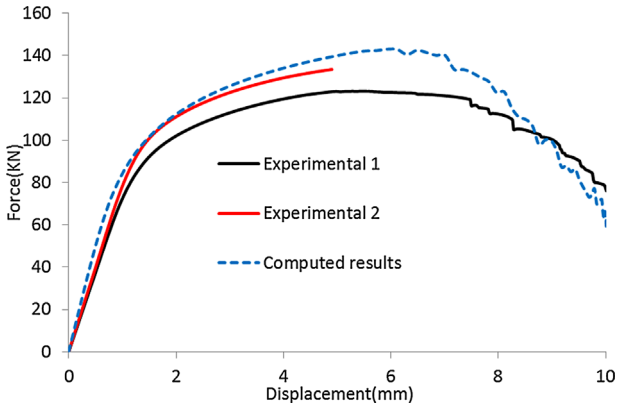

Fig. 6. Comparison of the computed results and experimental results for the quasi-static compression tests for the cellular structure.

cell,[54] and experimentally by testing cellular materials under shear or compressive loads.[8,12,14,17,19]

5.1. Impact Modeling of Truss Structure and Solid Block

As for the quasi-static deformations studied above, transient deformations of a quarter of the cellular structure and a $25.4 \times 25.4 \times 31.9$ mm^3 solid plate of the same areal density were analyzed with ABAQUS/Explicit with a uniformly distributed time-dependent pressure of peak magnitude 500 MPa applied on the top surface. The 31.9 mm high solid plate was discretized into 250,000 eight-node brick elements (C3D8R) with one-point integration rule. The same contact algorithm and the element deletion technique as that for the quasi-static deformations studied above were employed.

5.2. Results and Discussion for the Impact Loading

The work done by the applied pressure loading during deformations of the cellular (solid) structure equaled 64.9 J (45.1) of which 25.7 J (41.9) were used to elastically and plastically deform the structure and 39.6 J (3.3) to increase the kinetic energy of the structure. It is thus clear that the cellular structure is more severely deformed than the solid plate that should also be evident from the deformed shapes exhibited in Figure 7. Whereas no element failed in the solid block, nearly half of the trusses in the cellular structure failed. However, the bottom plate of the cellular structure remained intact. Due to the reaction force exerted by the bottom rigid plate supporting the structures, the cellular and the solid structures bounce upwards at 300 and 50 μs, respectively, as indicated by the plot in Figure 8 of the time histories of the reaction force. The peak force (283 kN) exerted on the rigid supporting plate by the solid structure is considerably more than that (36 kN) exerted by the cellular structure, thereby providing significantly more protection to the structure to which they are bonded. Also, the impulse transferred to the substrate by the cellular structure is much less than that transmitted by the solid structure.

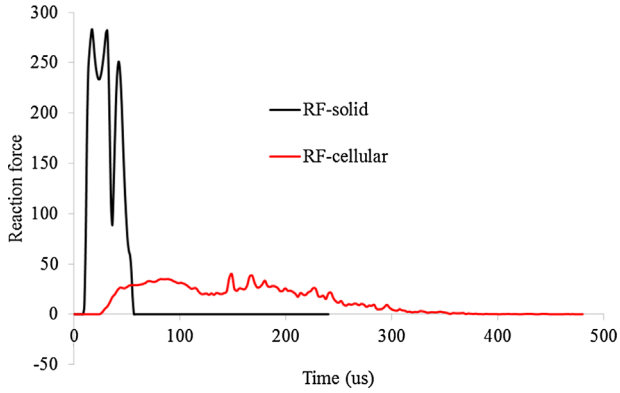

Fig. 8. Reaction forces applied on structure by the rigid plate supporting the structures.

6. Conclusions and Recommendations for Future Work

In this paper, a method for the creation of lightweight, metal cellular structures was presented utilizing the capabilities of Binder Jetting and traditional casting techniques. Binder Jetting is advantageous in that it is scalable and relatively inexpensive, and the printed powders used for casting allow processing of many different alloys. A proof-of-concept octet truss structure with fully homogeneous sandwich panels was manufactured using the proposed Binder Jetting process. The resulting part quality, while partially dependent on part geometry, demonstrated that this method is capable of producing lightweight cellular structures with designed mesostructure through metal casting.

Quasi-static and transient deformations of the cellular and solid structures were studied by using values of material parameters determined from the test data and the commercial

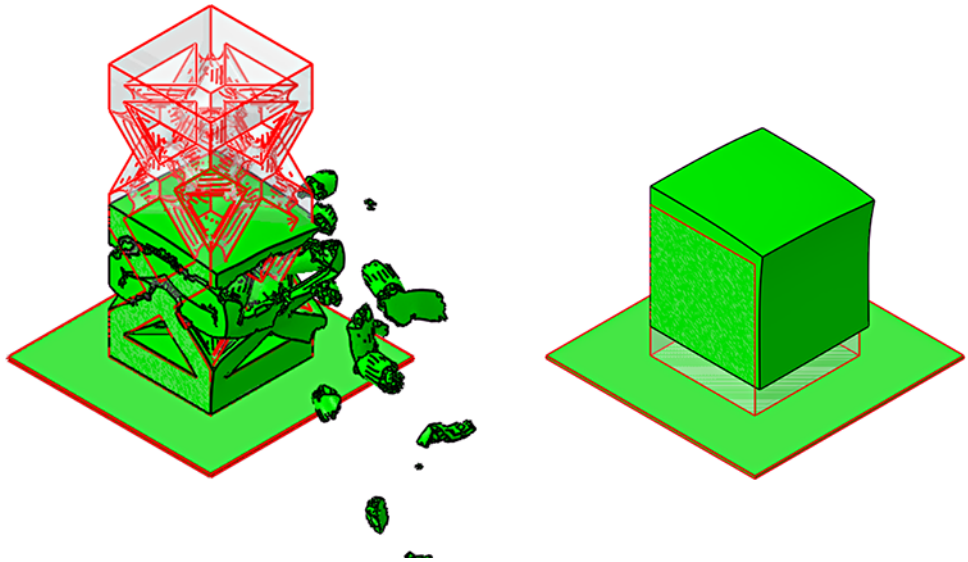

Fig. 7. Undeformed (red lines) and deformed (black lines) shapes of the cellular structure and the solid block at time = 480 μs.

software ABAQUS. For the same time-dependent pressure load applied on the top surfaces of the two structures with their bottom surfaces supported on smooth rigid plates, the total force exerted on the rigid plate by the cellular and the solid structures equaled 283 and 36 kN, respectively. Furthermore, the total impulse transferred by the cellular structure to the rigid plate is considerably less than that by the solid structure.

For future work, efforts will be focused on combining topology optimization with the proposed Binder Jetting process. Using topology optimization during the initial digital mold creation phase will allow for structures that are tailored to perform optimally under certain loading conditions. In addition, efforts will be undertaken to analytically model the flow of the molten metal through the mold, ensuring that the final parts are poured and completely filled, regardless of geometry. Modeling of deformations under quasi-static and impact loads will be used to optimize the design of cellular structures for minimizing the momentum and the peak pressure transferred to the substrate being protected by the cellular structure. Collaboration with outside sources will be sought for tests under blast loads. Additionally, printing the entire mold including gating system, core, and outer mold assembly will provide better geometrical tolerances. The resultant part will lead to less error between analytical and quasistatic results.

Received: November 21, 2014
Final Version: February 16, 2015
Published online: March 11, 2015

[1] J. Banhart, *Memb. J. Miner. Met. Mater. Soc.* **2000**, *52*, 22.
[2] J. Banhart, D. Weaire, *Phys. Today* **2002**, *55*, 37.
[3] A. G. Evans, J. W. Hutchinson, M. F. Ashby, *Prog. Mater. Sci.* **1999**, *43*, 171.
[4] A. G. Evans, J. W. Hutchinson, N. A. Fleck, M. F. Ashby, H. N. G. Wadley, *Prog. Mater. Sci.* **2001**, *46*, 309.
[5] C. C. Seepersad, R. S. Kumar, J. K. Allen, F. Mistree, D. L. Mcdowell, *J. Comput. Mater. Des.* **2004**, *11*, 163.
[6] S. C. Thompson, H. Muchnick, H. Choi, D. Mcdowell, in *Multidiscip. Anal. Optim. Conf.*, **2006**, 1.
[7] C. C. Seepersad, J. K. Allen, D. L. McDowell, F. Mistree, *J. Mech. Des.* **2006**, *128*, 1285.
[8] H. Wadley, *Compos. Sci. Technol.* **2003**, *63*, 2331.
[9] D. T. Queheillalt, Y. Murty, H. N. G. Wadley, *Scr. Mater.* **2008**, *58*, 76.
[10] M. F. Ashby, A. G. Evans, N. A. Fleck, J. W. Gibson, J. W. Hutchinson, H. N. G. Wadley, in *Metal Foams: A Design Guide*, Butterworth-Heinemann, Woburn, MA **2000**.
[11] J. W. Gibson, M. F. Ashby, in *Cellular Solids: Structures and Properties*, Cambridge University Press, Cambridge, *UK* **1997**.
[12] L. Mori, S. Lee, Z. Xue, A. Vaziri, D. Queheillalt, K. Dharmasena, H. Wadley, J. Hutchinson, H. Espinosa, *J. Mech. Mater. Struct.* **2007**, *2*, **1981**.
[13] D. Queheillalt, V. Deshpande, H. Wadley, *J. Mech. Mater. Struct.* **2007**, *2*, 1657.
[14] P. Moongkhamklang, H. N. G. Wadley, *Adv. Eng. Mater.* **2010**, *12*, 1111.
[15] Jonathon Aerospace Materials, www.jamcorp.com, **2004**.
[16] M. V. Nathal, J. D. Wittenberger, M. G. Hebsur, P. T. Kantzos, D. L. Krause, in *10th Int. Symp. Superalloys*, Champion, PA **2004**.
[17] B. D. J. Sypeck, H. N. G. Wadley, *Adv. Eng. Mater.* **2002**, *1028*, 759.
[18] A. Hattiangadi, A. Bandyopadhyay, in *Int. Solid Free. Fabr. Symp.*, **1999**, 319.
[19] S. Chiras, D. R. Mumm, A. G. Evans, N. Wicks, J. W. Hutchinson, K. Dharmasena, H. N. G. Wadley, S. Fichter, *Int. J. Solids Struct.* **2002**, *39*, 4093.
[20] A. Lyons, S. Krishnan, J. Mullins, M. Hodes, D. Hernon, in *Int. Solid Free. Fabr. Symp.*, Austin, TX **2009**, 749.
[21] O. Cansizoglu, D. Cormier, O. Harrysson, H. West, T. Mahale, in *Int. Solid Free. Fabr. Symp.*, Austin, TX **2006**, 209.
[22] M. Agarwala, D. Bourell, J. Beaman, H. Marcus, J. Barlow, *Rapid Prototyp. J.* **1995**, *1*, 26.
[23] D. T. Pham, C. J. Dimov, R. S. Gault, in *1st Int. Conf. Adv. Res. Virtual Rapid Prototyp.*, Leiria, Portugal **2003**, 107.
[24] W. Brooks, C. Sutcliffe, W. Cantwell, P. Fox, J. Todd, R. Mines, in *Int. Solid Free. Fabr. Symp.*, Austin, TX **2005**, 231.
[25] J. Kobliska, P. Ostojic, X. Cheng, X. Zhang, H. Choi, Y. Yang, X. Li, in *SFF Symp.*, **2005**, 468.
[26] L. Yang, O. Harrysson, H. West II, D. Cormier, in *Int. Solid Free. Fabr. Symp.*, Austin, TX **2011**, 464.
[27] C. B. Williams, F. Mistree, D. W. Rosen, in *ASME IDETC Des. Manuf. Life Cycle Conf.*, Long Beach, CA **2005**, 1.
[28] M.F. Zaeh, G. Branner, *Prod. Eng.* **2009**, *4*, 35.
[29] M. Shiomil, K. Osakada, K. Nakamura, F. Yamashita, F. Abe, *CIRP Ann.-Manuf. Technol.* **2004**, *53*, 195.
[30] K. Mumtaz, P. Vora, N. Hopkinson, in *Int. Solid Free. Fabr. Symp.*, Austin, TX **2011**, 55.
[31] Z Corporation, Burlington, MA USA, *ZCast® 501 Direct Metal Casting Design Guide*, **2009**.
[32] ExOne, N. Huntingdon, PA USA, *S-Max Furan*, www.exone.com/en/materialization/systems/m-flex, **2014**.
[33] ExOne, N. Huntingdon, PA USA, *M-Flex*, www.exone.com/en/materialization/systems/s-max, **2014**.
[34] Voxeljet AG, Friedburg Germany, Large-format sand moulds for metal casting, www.voxeljet.de/fileadmin/Voxeljet/Services/Sand_casting_2012.pdf, **2012**.
[35] M. Chhabra, R. Singh, *Rapid Prototyp. J.* **2011**, *17*, 328.
[36] M. Stankiewicz, G. Budzik, M. Patrza, M. Wieczorowski, M. Grzelka, H. Matysiak, J. Slota, *Arch. Foundry Eng.* **2010**, *10*, 405.
[37] J. Campbell, in *Castings Practice: The Ten Rules of Castings*, Butterworth-Heinemann, Oxford, UK **2004**.

[38] C. B. Williams, F. Mistree, D. W. Rosen, in *Int. Solid Free. Fabr. Symp.*, Austin, TX **2005**, 1.
[39] E. Bassoli, E. Atzeni, *Rapid Prototyp. J.* **2009**, *15*, 238.
[40] N. Mckenna, S. Singamneni, O. Diegel, D. Singh, T. Neitzert, J. S. George, A. R. Choudhury, P. Yarlagadda, in *9th Glob. Congr. Manuf. Manag.*, Surfers Paradise, Australia **2008**, 12.
[41] S. S. Gill, M. Kaplas, *Int. J. Adv. Manuf. Technol.* **2010**, *52*, 53.
[42] S. S. Gill, M. Kaplas, *Mater. Manuf. Process.* **2009**, *24*, 1405.
[43] M. Chhabra, R. Singh, *Rapid Prototyp. J.* **2012**, *18*, 458.
[44] E. Bassoli, A. Gatto, L. Iuliano, M. G. Violante, *Rapid Prototyp. J.* **2007**, *13*, 148.
[45] P. R. Beely, *Foundry Technology*, **2001**.
[46] N. A. Meisel, C. B. Williams, A. Druschitz, in *Int. Solid Free. Fabr. Symp.*, **2012**.
[47] D. A. Snelling, R. Kay, A. Druschitz, C. B. Williams, in *Int. Foundry Res.*, **2014**.
[48] G. Budzik, *Arch. Foundry Eng.* **2007**, *7*, 65.
[49] J. Kawola, *ZCast Direct Metal Casting: From Data to Cast Aluminum in 12 hours*, www.3dprint.no/images/Nyheter_info/ZCast%20info.pdf, **2003**.
[50] netfabb GmbH, Lupburg Germany, netfabb Version 4.9, www.netfabb.com, **2011**.
[51] F. P. Schleg, *Technology of Metalcasting*, American Foundry Society, Schaumburg, IL **2003**.
[52] D. Snelling, C. B. Williams, A. Druschitz, in *Int. Solid Free. Fabr. Symp.*, **2014**.
[53] Dassault Systèmes, Abaqus Version 6.11, www.3ds.com, **2014**.
[54] V. S. Deshpande, N. A. Fleck, M. F. Ashby, *J. Mech. Phys. Solids* **2001**, *49*, 1747.

